Original Article

Biomechanical evaluation of interlocking nail and locking compression plating for stabilization of ovine critical-sized segmental tibia defects

Drew W. Koch[1]^, James W. Johnson[2]^, Quinn E. Smith[2], Chloe Brekhus[2], Benjamin C. Gadomski[2]^, Ross H. Palmer[1,3], Jeremiah T. Easley[1,3], Brad B. Nelson[1,3]^

[1]Department of Clinical Sciences, Colorado State University, Fort Collins, CO, USA; [2]Orthopaedic Bioengineering Research Laboratory, C. Wayne McIlwraith Translational Medicine Institute, Colorado State University, Fort Collins, CO, USA; [3]Preclinical Surgical Research Laboratory, C. Wayne McIlwraith Translational Medicine Institute, Colorado State University, Fort Collins, CO, USA

Contributions: (I) Conception and design: DW Koch, BC Gadomski, JT Easley, BB Nelson; (II) Administrative support: None; (III) Provision of study materials or patients: None; (IV) Collection and assembly of data: All authors; (V) Data analysis and interpretation: DW Koch, BB Nelson; (VI) Manuscript writing: All authors; (VII) Final approval of manuscript: All authors.

Correspondence to: Brad B. Nelson, DVM, PhD, DACVS. 300 W. Drake Road, Colorado State University, Fort Collins, CO 80523, USA.
Email: Brad.nelson@colostate.edu.

Background: Segmental large volume bone loss resulting from fracture or osseous neoplasia is a major challenge to orthopedic surgeons and there is an ongoing quest to identify treatments that optimize healing. To advance treatment, large animal translational models—such as the ovine critical-sized tibia defect model—are instrumental for testing of novel scaffolds for bone regeneration. However, little standardization in the implants utilized for defect stabilization has been determined and current commercially available implants may be inadequate to replicate the strength of the native tibia. We hypothesize that a 10-mm interlocking nail (ILN) would be stiffer in axial, bending, and torsional loading than its 8-mm counterpart and would be stiffer in axial and torsional loading compared to a 4.5-mm broad locking compression plate (LCP).

Methods: Tibias were harvested from 24 ovine hind limbs from skeletally mature ewes euthanized for reasons unrelated to this study and were randomized to treatment group. An *ex vivo* comparison of a novel 10-mm angle-stable non-tapered ILN was compared to a commercially available 8-mm angle-stable tapered ILN and a broad LCP in an ovine critical-sized (5-cm) tibia defect model. Axial stiffness, torsional stiffness, and bending stiffness were determined in control intact tibia and tibial constructs in the three treatment groups. Following implantation, radiography was performed in all limbs and tibia length and cortical and medullary cavity diameter were measured. Comparisons between groups were assessed with a one-way analysis of variance. Significance was set at $P<0.05$.

Results: The 10-mm ILN in tibia containing a 5-cm ostectomy gap most closely replicated the structural properties of intact tibia compared with other constructs. The 10-mm ILN had significantly stronger torsional ($P<0.001$) and bending ($P=0.002$) stiffness than the 8-mm ILN, and was significantly stronger than the LCP in axial ($P=0.04$) and torsional ($P=0.01$) stiffness.

Conclusions: A 10-mm ILN used to stabilize an ovine critically-sized tibia defect most closely mimicked the structural properties of the intact tibia when compared to a 8-mm ILN or broad LCP. Further *in vivo* testing will aid in determining which stabilization method is best suited for testing of novel tissue engineering and bone healing studies.

Keywords: Sheep; translational; orthopedic; fracture; bone

^ ORCID: Drew W. Koch, 0000-0001-9267-2995; James W. Johnson, 0000-0001-7465-3854; Benjamin C. Gadomski, 0000-0003-1434-0551; Brad B. Nelson, 0000-0002-0205-418X.

Submitted Oct 04, 2022. Accepted for publication Feb 08, 2023. Published online Mar 15, 2023.
doi: 10.21037/atm-22-4886
View this article at: https://dx.doi.org/10.21037/atm-22-4886

Introduction

Large amounts of segmental bone loss following fracture or osseous neoplasia is a major orthopedic challenge. Restoration of the large void of bone lost requires longer periods of secondary fracture healing than small defects or fractures that can be reconstructed. There is an ongoing quest for new bone graft scaffolds and tissue engineering strategies that promote and hasten bone regeneration (1-3). Large animal translational models are critical tools for bone healing research as they enable standardization and consistency of the investigated therapies. Additionally, large animal translational models, including the ovine tibia critical-defect model, have similar haversian bone structure and long bone size to that of humans (3-6). Therefore, utilization of ovine models enhances the likelihood that novel bone regeneration therapies tested in a preclinical setting can be successfully translated to human clinical medicine. Despite the variety of tissue engineering approaches being investigated, there is no consensus on how best to stabilize and promote healing of these tibial bone defects in sheep.

Implants used to stabilize large bone defects have included external fixators, locking compression plates (LCPs), or interlocking nails (ILNs) (5,7-9). However, there is a lack of consistency in stabilization techniques used in ovine tibia defects (5). Because of the inability to restrict postoperative activity in sheep, it is crucial to choose an implant suited to the loading experienced *in vivo* and one that also allows appropriate mechanobiological feedback (i.e., fracture gap strain) to accurately replicate the native fracture healing environment. This ensures meaningful conclusions can be made from *in vivo* data, and therefore, improves clinical translation.

The study objective was to compare the biomechanical properties of cadaver ovine tibias with critical-sized ostectomy defects to determine which implant construct best restored the stiffness of the intact (INT) tibia. We hypothesized that a 10-mm cylindrical ILN would be stiffer in axial, bending, and torsional loading than its commercially available 8-mm centrally tapered counterpart, and would be stiffer in axial and torsional loading compared to a broad LCP. We present the following article in accordance with the ARRIVE reporting checklist (available at https://atm.amegroups.com/article/view/10.21037/atm-22-4886/rc).

Highlight box

Key findings

- A 10-mm interlocking nail when used to stabilize a tibial ostectomy defect most closely mimicked the structural properties of the intact tibia when compared to an 8-mm interlocking nail or broad locking compression plate.

What is known and what is new?

- There are a variety of implants used in ovine translational bone research to test new scaffolds and bone healing therapies. The decision of which implants used to stabilize ostectomy defects is not standardized.
- This study directly compares the *ex vivo* mechanical stiffness of interlocking nails and locking compression plate used to stabilize tibia ostectomy defects with intact tibias under the three principal loading conditions.

What is the implication, and what should change now?

- These data can be used for researchers that use tibia osteotomy models to help determine which stabilization method is best suited for their use.

Methods

As cadaver tissues were used and no *in vivo* experimentations were performed, review by the Animal Care and Use Committee at our institution was not required.

Perioperative assessment

Twenty-four ovine hind limbs from skeletally mature (>3 years) Rambouillet crossbred ewes were procured from animals sacrificed in unrelated studies. Limbs were frozen at –20 ℃ and each limb was thawed at room temperature over 24 hours prior to implant placement and mechanical testing. Limbs were randomly allocated to one of four groups (6 per group) using a random number generator and using a blocking structure to ensure the same number of limbs per group (random.org). One group included INT (no implant) tibia (n=6) while the remaining groups had a 5-cm ostectomy performed in the mid-diaphysis and

were stabilized with either an angle-stable 8-mm thickness × 210-mm length tapered ILN (ILN-8, Biomedtrix, Whippany, NJ, USA, n=6), an angle-stable 10-mm thickness × 210-mm length non-tapered ILN (ILN-10, Biomedtrix, n=6), or a 4.5-mm broad 11-hole LCP (Synthes, Warsaw, IN, USA, n=6). The ILN-10 was custom manufactured (Biomedrix) to provide a potentially stiffer alternative to the centrally tapered ILN-8. Radiography (craniocaudal and lateromedial projections) with a radiopaque ruler was performed on all limbs after implantation. Measurement of tibia length, medullary cavity diameter, and cortical diameter were performed by a single author (DWK) following implant placement using the craniocaudal radiographic view and a free, open-source DICOM medical image viewer (Horos™, v3.3.6, horosproject.org). Tibial length was measured from the medial tibial plateau to the medial malleolus at the level of the articulation of the medial tibia cochlea with the medial trochlear ridge of the talus. Medullary cavity and cortical diameter were measured at the same location immediately distal to the ostectomy site. Radiographic measures of cadaveric ovine tibia revealed that this site is the smallest medullary cavity diameter that intramedullary devices would need to pass through (unpublished data).

Surgical approach

The soft tissues were maintained for creation of the ostectomy and implant placement to ensure the implantation procedure could be replicated *in vivo*. A linear incision was made through the skin, subcutaneous tissue and periosteum on the medial aspect of the tibia to expose the mid-diaphysis. Tibial length was measured from the medial tibial plateau to the medial malleolus as described above. Using this measurement, the middle of the diaphysis was demarcated and a 5-cm ostectomy centered at this location was created (except for the INT group). The periosteum was reflected circumferentially, and the mid-diaphysis ostectomy was performed using an oscillating saw. A custom cylindrical guide with central channel to accommodate the ILNs (10) was placed into the ostectomy void to ensure the gap remained at 5-cm length during ILN or LCP placement.

With the cylindrical guide in place, the tibia was reduced, maintained in anatomic alignment and the ILNs were placed in a normograde fashion (11). For the ILN-8, the stifle was flexed and a stab incision with a #10 blade was made in the soft tissues medial and adjacent to the patellar ligament to access the proximal tibia. A 4.3-mm drill bit was used to direct placement of the ILN cranial on the medial tibial plateau. A dedicated awl was used to enlarge the hole and a hand reamer used to remove adipose marrow, which was extended distad into the distal tibial metaphysis (Biomedtrix, Whippany, NJ, USA). To facilitate placement of the ILN-10, an additional step using a 10-mm drill bit was required to enlarge the hole in the proximal tibia plateau. A reamer removed adipose tissue in the medullary canal to accommodate the ILN. The insertion handle with nail extension was used to advance each ILN until it stopped at the distal tibial metaphysis. Endosteal reaming was not performed. Reduction and rotational alignment of the tibia were confirmed by direct visualization. An alignment drill guide was attached over the insertion handle to align the outer drill sleeves with the ILN bolt holes. Starting at the proximal tibia and moving distad, the drill holes were placed in the following sequence. The cis cortical pilot hole was drilled using a 4.3-mm drill bit until the ILN was reached. The feeler handler was introduced into the cis pilot hole to ensure the threaded cannulations within the nail could be felt, confirming ILN alignment. Next, the trans 3.2-mm cortical pilot hole was drilled through the ILN cannulation. An alignment post was placed to maintain ILN and pilot hole alignment. Then, the remaining three holes were drilled using this sequence from proximal to distal. Each alignment post was individually removed, and a positive profile threaded bolt inserted and tightened. Rotational stability was confirmed after all bolts were placed.

To ensure ostectomy gaps were consistent in the LCP group, alignment of the LCP on the tibia was confirmed prior to ostectomy. After the 5-cm ostectomy was marked, a 4.5-mm broad 11-hole LCP was placed on the medial tibia. The three middle holes of the LCP were aligned over the planned ostectomy. Then, 4.3-mm threaded drill guides were placed in holes 4 and 8 (numbered from proximal to distal) of the LCP and a 4.3-mm drill bit was used to drill bi-cortical pilot holes into the proximal and distal segments of the tibia, respectively. The LCP was removed and the 5-cm ostectomy was performed as described earlier. The LCP was replaced on the medial aspect of the tibia. Self-tapping 5.0-mm locking screws were placed into previously drilled pilot holes to align the LCP on the tibia. Threaded drill sleeves were used to align the pilot holes for the remaining screws. Locking screws (5-mm) were placed in all holes except those at the level of the ostectomy (4 screws each in the proximal and distal segments) (9). Three additional 5.0-mm locking screws were placed into

the open holes of the LCP (holes 5 through 7) to ensure there would not be a focal area of stress placed on the plate during biomechanical testing. *In vivo*, locking screw caps would be used to avoid impacting scaffolds placed within the ostectomy defect while preventing focal stresses on the plate.

Biomechanical analysis

The proximal and distal ends of each tibia were mounted in a quick-cure resin (Smooth-Cast 320, Smooth-On, Inc.) extending just into the proximal and distal metaphysis, respectively. Two small wood screws were placed in the proximal and distal articular surfaces at each end of the tibia to increase torsional purchase within the bone-resin interface. For the mounting process, the resin was molded to fit with a custom-fabricated testing rig designed to hold the tibia-resin construct during biomechanical testing. Non-destructive biomechanical testing was performed using a servohydraulic testing machine (MTS Landmark, MTS Systems Corp.). Biomechanical testing consisted of three tests including: axial compression [5 linear cycles, 500 N limit, (0.1 mm/s)], torsion [5 linear cycles, 5 Nm limit, (0.1 deg/s)], and four-point bending tested in the cranial-to-caudal direction [5 linear cycles, 5 Nm bending moment limit, (0.1 mm/s)]. Torsion was tested in the lateral direction for each sample where the tibial plateau rotated laterally relative to the tarsocrural joint. Outcome parameters included axial stiffness (N/mm), torsional stiffness (Nm/deg), and bending stiffness (N/mm). These parameters were calculated by measuring the slope of the load-displacement curve generated for each construct. To allow for normalization of viscoelastic effects during testing, stiffness values were calculated from the loading portion of the fifth cycle of testing.

Statistical analysis

Data were reported as mean and standard deviation. Data normality was assessed using Shapiro-Wilk tests and graphically using quantile-quantile plots. Statistical comparisons were made between groups (tibias) using a one-way ANOVA (analysis of variance) following confirmation of data normality and equal variance assumptions, with critical alpha of 0.05 and a Tukey post-hoc test (GraphPad Prism, v9.2, La Jolla, California).

Results

Representative radiographs of each group are shown in *Figure 1*. Radiographic measures of tibia length, medullary cavity diameter, and cortical diameter are reported in *Table 1*.

Axial stiffness of the ILN groups most closely matched the INT group (ILN-8: 6% decrease, ILN-10: 10% increase), while the LCP group was much lower than the INT group (53% decrease) (*Figure 2*). Axial stiffness in the LCP group was significantly lower than the ILN-10 group (P=0.04). Bending stiffness of the ILN-10 group most closely matched the INT group (18% decrease). The ILN-8 group exhibited lower bending stiffness as compared to the INT group (55% decrease). The LCP group demonstrated a 43% increase in bending stiffness as compared to the INT group (*Figure 2*). Bending stiffness of the ILN-8 group was significantly lower than INT (P<0.001), ILN-10 (P<0.002), and LCP (P<0.001) groups. While the ILN-10 group had significantly lower torsional stiffness (47% decrease, P<0.001) than the INT group, it was the group that most closely matched the INT tibia compared to ILN-8 and LCP. The ILN-8 and LCP groups both had significantly decreased torsional stiffness compared to INT tibia at a 75% decrease (P<0.001) and 51% decrease (P<0.001), respectively. Torsional stiffness in the ILN-8 group was significantly lower than the LCP group (P<0.001) and the ILN-10 group (P<0.001). Torsional stiffness in the LCP group was significantly lower than the ILN-10 group (P=0.01).

Discussion

Under physiologic loading, the ovine tibia has been shown to be largely deformed in torsion (62% of total load) and bending (33%) and less in axial compression (5%) (12). We demonstrate that use of the ILN-10 exhibited structural properties most similar to the intact ovine tibia. Specifically, the ILN-10 group exhibited properties within 10% axial stiffness, within 34% torsional stiffness, and within 18% bending stiffness of intact tibias. The LCP group approximated intact tibias in torsion and bending; however, it was inferior in axial compression. While the ILN-8 group closely matched the intact group in axial stiffness, other loading conditions (torsion and bending) that are more likely to lead to failure *in vivo* revealed that the ILN-8 was inferior to other constructs evaluated. In support of our

Figure 1 Representative craniocaudal radiographs of ovine tibia in each group following implant placement and prior to mechanical testing. INT limbs did not undergo critical-size defect creation or implant placement. Defects in tibia were created prior to implant placement in ILN-8 and ILN-10 groups but after placement and removal of implants in LCP-treated limbs. All screw holes of the LCP were filled to prevent focal areas of increased stress at the middle of the plate during testing. INT, intact; ILN-8, 8-mm interlocking nail; ILN-10, 10-mm interlocking nail; LCP, locking compression plate.

Table 1 Mean (standard deviation) measurements of tibia length, medullary cavity diameter, and cortical diameter for tibia in INT, LCP, ILN-8 and ILN-10 (n=6/group) treatment groups

Measurement	INT	LCP	ILN-8	ILN-10
Length (cm)	23.10 (1.99)	23.05 (1.02)	24.12 (0.658)	25.14 (1.80)
Medullary cavity diameter (mm)	10.19 (0.496)**	10.57 (1.11)*	11.00 (0.881)	12.32 (0.672)*,**
Cortical diameter (mm)	19.96 (0.678)	19.64 (1.26)	20.48 (0.624)	20.82 (1.55)

Groups with the same superscripts identify a significant difference (*P=0.007 or **P=0.001) between groups. INT, intact; LCP, locking compression plate; ILN-8, 8-mm interlocking nail; ILN-10, 10-mm interlocking nail.

hypothesis, the ILN-10 was significantly stiffer in bending and torsion than the ILN-8, and the average axial stiffness of the ILN-10, while higher, was not significantly higher than the ILN-8. Moreover, the ILN-10 was significantly stiffer in axial and torsional loading than the LCP.

Previous work has implemented various sizes of intramedullary nails to develop translational large animal models of bone nonunion, to assess their ability to stabilize fractures, or for testing of novel scaffolds for bone healing (5,7,10,13-17). These studies standardly implement ovine or canine tibias or femurs following ostectomy to assess outcomes. Lozada-Gallegos *et al.* implanted a 9-mm ILN in an *in vivo* ovine nonunion fracture model (11). While a much smaller ostectomy was used (5-mm), the 9-mm ILN was able to maintain animal comfort and ostectomy gap without reported implant breakage for the 8-week study

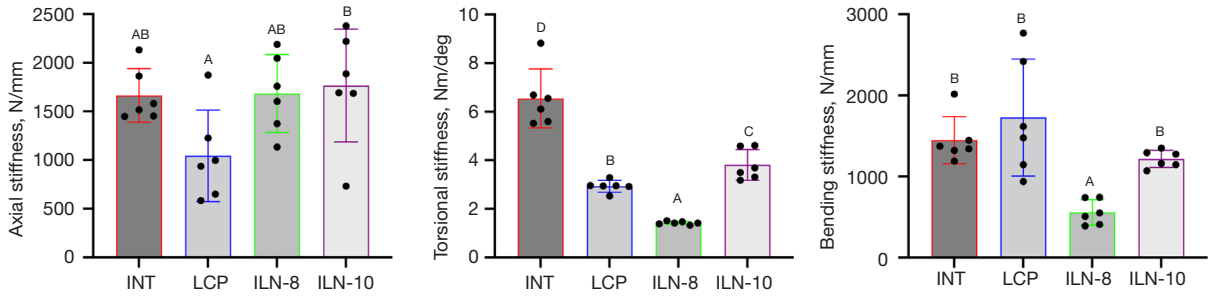

Figure 2 Critical-size tibia defects treated with an ILN-10 more closely mimic the structural properties of INT tibia. Outcome parameters included axial stiffness (N/mm), torsional stiffness (Nm/deg), and bending stiffness (N/mm) and were calculated by measuring the slope of the load-displacement. Normalization of viscoelastic effects during testing were calculated from the fifth cycle of testing. Differences in letter indicate a significant statistical difference (P<0.05) as measured by one-way ANOVA. N, Newton; INT, intact; LCP, locking compression plate; ILN-8, 8-mm interlocking nail; ILN-10, 10-mm interlocking nail; ANOVA, analysis of variance.

period. When an 8-mm nail (non-tapered) was used to stabilize a 5-cm ostectomy, Pluhar *et al.* found it to be of sufficient stiffness for animals through the duration of the study (10).

While a non-tapered 8-mm ILN has been used successfully, a subsequent *in vivo* study from our group using a newly designed tapered ILN-8 and ostectomy model caused severe bending of the ILN that required additional stabilization (unpublished data). The designed centrally tapered hourglass profile of the ILN-8 is proposed to limit interference with the endosteal surface, thereby avoiding iatrogenic damage during placement, optimizing revascularization at the fracture site, and increasing construct compliance (18,19). Despite the ILN-8 being engineered to address these potential pitfalls, it also focuses the bending force at the center of the ILN, which coincidently is at the center of the ostectomy gap in this model. This leads to construct weakness at the ostectomy site, particularly when torsion or bending forces are applied. The ILN-8 design has been used successfully for repair of clinical fractures in dogs and even in two calves that had similar weights as adult sheep (20). However, in those two calves, the tibial cortices either could be reconstructed and held in alignment with cerclage wire, or the fracture was located in the proximal tibia and was not directly opposite the center of the ILN. Adjunctive stabilization techniques should be considered when the tapered portion of an ILN is at the same level as the segmental or unreconstructed bone defect in larger animals or when postoperative exercise cannot be restricted.

There are implant-specific differences between ILNs and LCPs in their composition and the location where they can be applied to the tibia, which can influence their mechanical behavior (3,9). ILNs are placed within the medullary cavity, whereas LCPs are placed on the cortical/periosteal surface. Implant stiffness is a representation of the material to resist deformation. It is dependent on Young's modulus of the material, the cross-sectional shape and size (and related area and polar moment of inertia), and its working length (21). It would have been interesting to test multiple sizes of each implant using this study design. However, considering the limited availability of commercial implants for use in animals, we aimed to focus this study on how the stiffness of each implant construct relates to an intact tibia under the three main loading conditions. To limit influences on testing, all explants were mounted at the proximal and distal ends of the tibia excluding the ILN, LCP or their associated components. Forces applied through mechanical testing were done only through the bone.

There are benefits and limitations of ILN or LCP use (20-22). Although the LCP counteracted bending and torsion to a similar degree as the ILN-10, some intricacies of LCP placement require consideration and might make them less suitable implants for a particular situation. While LCPs avoid the articular surface (and related complications), larger incisions are typically needed to expose the bone unless newer minimally invasive approaches are performed. Broad plates in particular require precise alignment to ensure screws enter the medullary cavity and are not placed solely through the cortex creating focal stress in the bone and subsequent fracture. Conversely, ILNs are placed through the proximal articular surface, large incisions are not required, and in certain instances are easier to utilize in fracture repair compared to LCPs. Radiographic

assessment of bone healing at the defect site is subjectively easier with an ILN than LCP as the plate is superimposed over the bone void or fracture gap when the radiographic beam is parallel to the screw trajectory. Despite our results indicating the LCP had lower axial stiffness and slightly (albeit significantly) lower torsional stiffness than the ILN-10 group, it may also be suitable for stabilization of segmental defects. Other studies using variations of plate fixation have been used successfully in caprine and ovine *in vivo* models (6,9,23,24).

Additionally, properties of implanted scaffolds will impact their ability to be used with ILNs or LCPs. Scaffolds placed in conjunction with normograde ILN stabilization require an extra incision at the fracture site. Since the ILNs span the center of the bone, scaffolds also need to fit around the ILN to occupy the ostectomy (or bone void) gap. Tissue engineered malleable and 3D printed scaffolds are molded or designed with a central channel to fit around the ILN (3). Since LCPs are placed on the cortical surface, they do not interfere with the center of the bone and placement of the scaffold has less restrictions in ostectomy gap models. Additionally, with LCPs, the screw holes directly opposite the scaffold are left empty or are filled with screw caps (no screw shaft) to avoid an area of stress concentration on the plate.

A clear advantage of the ILN-10 over the ILN-8 is its increased diameter and filling of the medullary cavity, which increases implant stiffness and more effectively counteracts the biomechanical forces placed upon a bone containing a critical-sized defect (20,23). Additionally, without the hourglass taper of the ILN-8, the ILN-10 lacks a focal area of weakness during limb loading. These data support the ability of the ILN-10 to return the ostectomized tibia to its intact stiffness, more so than the ILN-8 and LCP. Therefore, if the tibia medullary cavity can accommodate the ILN-10, it appears to be a more appropriate choice of implant than the others tested for bone healing models or utilizing critical-sized defect models in sheep. Despite these results, further testing is required to ensure these findings are applicable to *in vivo* conditions.

The sizes of implants to be used in this study were determined from preliminary testing. Despite this preliminary work, the medullary cavity in some tibias in this study was too small to accommodate the 10-mm ILN, specifically where the tibia becomes more oval shaped in the distal diaphysis and metaphysis (flattened on cranial and caudal aspects). Sheep breeds will vary in tibia size and shape, and slight adjustments may be required to accommodate the 10-mm ILN when applying these results to future studies. Preoperative radiographic planning will ensure proper fit. Alternatively, reaming of the endosteal surface would slightly enlarge the medullary cavity. While reaming is an acceptable method for *in vivo* use, we avoided this to enable consistency in this *ex vivo* experimental study. Tight fitting ILNs could predispose to cortical fissures, even though this is a recognized complication with smaller ILNs. Pluhar *et al.* used 8-mm ILNs and reported five of 26 limbs required cerclage wiring to prevent propagation of fractures post-implantation (10). The authors believe risks of overly large ILNs can be abrogated by performing preoperative radiographs and determining medullary cavity dimensions prior to implementation.

Critical-size bone defects are conventionally defined as the minimum amount of bone loss that will not heal unassisted in the lifetime of the animal, one with less than 10% bony regeneration, or defects 1.5 to 2 times the diaphyseal diameter (10,25). However, ovine bone models have a remarkable capacity for healing and the definition of critical-sized defect is questioned (1). Nonetheless, a result of high energy trauma, neoplasia, or infection, the capacity for these defects to heal following surgical repair is often determined by the bone affected, extent of bone loss, and whether local therapy, such as autologous bone grafts, are pursued (1). The ovine model of critical-size bone defect is an established method to test novel implants and develop new therapies for bone healing because of the similarity in bone healing between sheep and humans (5,25). Our laboratories have implemented a model of a critical-sized ovine tibia defect to examine novel scaffolds and regenerative therapies to develop translational therapies for bone healing (3).

Measurements of the tibias revealed a range of medullary cavity widths, which were likely associated with individual variations in growth; tibias used in this study were all from skeletally mature ewes of the same breed. While no significant difference in tibia length or cortical diameter was measured between groups, limbs treated with the ILN-10 had a significantly larger medullary cavity than the intact control and LCP-treated limbs. Because limbs were randomized to treatment, this was unforeseen. It is possible that placement of the ILN-10 led to slight dilation of the medullary canal or the close apposition of the ILN with the endosteal surface falsely increased diameter measurements post-implantation. Even though there was no difference in cortical measurements—where the fixation points on the ILN (via bolts) and LCP (via locking screw heads) are

located—the difference in medullary diameter could have an unrecognized effect on our results.

A limitation of biomechanical testing of *ex vivo* specimens is the inability to replicate *in vivo* conditions where biomechanical forces act concurrently in multiple planes as well as at faster rates. Therefore, these statistical comparisons do not necessarily equate to biological differences and caution should be taken extrapolating findings to *in vivo* settings. Single cycle to failure testing was considered. However, these extreme, consistent, and relatively slow ramping loads are unlikely to be observed under *in vivo* conditions. Clinically, fractures typically occur due to acute (rapid) overload or accumulation of micro-stresses placed on implants with a lack of bone healing. By using similarly sized tibias and standardizing the ostectomy creation and implantation procedures, we were able to compare the different constructs consistently and directly. *In vivo*, the impact of stress shielding and impact to the vascular supply when using these implants were not investigated. Since none of these implants were significantly stiffer than intact tibia, we suspect they are not stiff enough in the face of a large 5-cm defect to lead to delayed or non-union.

Conclusions

In conclusion, we demonstrate that the ILN-10 provided an overall more robust return to the native structural properties of intact ovine tibia containing a 5-cm critical-sized defect compared to the ILN-8 and LCP. Future work should examine the ILN-10 in an *in vivo* critical-size defect study to further characterize its utility.

Acknowledgments

Funding: There was no proprietary interest or funding provided for this project. Stipend support for DW Koch was provided by NIH (No. 5T32OD011130).

Footnote

Reporting Checklist: The authors have completed the ARRIVE reporting checklist. Available at https://atm.amegroups.com/article/view/10.21037/atm-22-4886/rc

Data Sharing Statement: Available at https://atm.amegroups.com/article/view/10.21037/atm-22-4886/dss

Peer Review File: Available at https://atm.amegroups.com/article/view/10.21037/atm-22-4886/prf

Conflicts of Interest: All authors have completed the ICMJE uniform disclosure form (available at https://atm.amegroups.com/article/view/10.21037/atm-22-4886/coif). The authors have no conflicts of interest to declare.

Ethical Statement: The authors are accountable for all aspects of the work in ensuring that questions related to the accuracy or integrity of any part of the work are appropriately investigated and resolved. As cadaver tissues were used and no *in vivo* experimentations were performed, review by the Animal Care and Use Committee at our institution was not required.

References

1. Nauth A, Schemitsch E, Norris B, et al. Critical-Size Bone Defects: Is There a Consensus for Diagnosis and Treatment? J Orthop Trauma 2018;32 Suppl 1:S7-S11.
2. Roddy E, DeBaun MR, Daoud-Gray A, et al. Treatment of critical-sized bone defects: clinical and tissue engineering perspectives. Eur J Orthop Surg Traumatol 2018;28:351-62.
3. Yang YP, Gadomski BC, Bruyas A, et al. Investigation of a Prevascularized Bone Graft for Large Defects in the Ovine Tibia. Tissue Eng Part A 2021;27:1458-69.
4. Hillier ML, Bell LS. Differentiating human bone from animal bone: a review of histological methods. J Forensic Sci 2007;52:249-63.
5. Christou C, Oliver RA, Pelletier MH, et al. Ovine model for critical-size tibial segmental defects. Comp Med 2014;64:377-85.
6. Henkel J, Medeiros Savi F, Berner A, et al. Scaffold-guided bone regeneration in large volume tibial segmental defects. Bone 2021;153:116163.

7. von Pfeil DJ, Déjardin LM, DeCamp CE, et al. In vitro biomechanical comparison of a plate-rod combination-construct and an interlocking nail-construct for experimentally induced gap fractures in canine tibiae. Am J Vet Res 2005;66:1536-43.
8. Maissen O, Eckhardt C, Gogolewski S, et al. Mechanical and radiological assessment of the influence of rhTGFbeta-3 on bone regeneration in a segmental defect in the ovine tibia: pilot study. J Orthop Res 2006;24:1670-8.
9. Marcondes GM, Paretsis NF, Souza AF, et al. Locking compression plate fixation of critical-sized bone defects in sheep. Development of a model for veterinary bone tissue engineering. Acta Cir Bras 2021;36:e360601.
10. Pluhar GE, Turner AS, Pierce AR, et al. A comparison of two biomaterial carriers for osteogenic protein-1 (BMP-7) in an ovine critical defect model. J Bone Joint Surg Br 2006;88:960-6.
11. Lozada-Gallegos AR, Letechipia-Moreno J, Palma-Lara I, et al. Development of a bone nonunion in a noncritical segmental tibia defect model in sheep utilizing interlocking nail as an internal fixation system. J Surg Res 2013;183:620-8.
12. Gautier E, Perren SM, Cordey J. Strain distribution in plated and unplated sheep tibia an in vivo experiment. Injury 2000;31 Suppl 3:C37-44.
13. Seaman JA, Pluhar GE, Rose ND, et al. Evaluation of scintigraphy to assess incorporation of intercalary cortical bone grafts in sheep. Am J Vet Res 2009;70:1079-86.
14. Bloemers FW, Blokhuis TJ, Patka P, et al. Autologous bone versus calcium-phosphate ceramics in treatment of experimental bone defects. J Biomed Mater Res B Appl Biomater 2003;66:526-31.
15. Déjardin LM, Cabassu JB, Guillou RP, et al. In vivo biomechanical evaluation of a novel angle-stable interlocking nail design in a canine tibial fracture model. Vet Surg 2014;43:271-81.
16. Wilson DJ, Morgan RL, Hesselden KL, et al. A single-channel telemetric intramedullary nail for in vivo measurement of fracture healing. J Orthop Trauma 2009;23:702-9.
17. White AA, Kubacki MR, Samona J, et al. Removal torque of nail interlocking screws is related to screw proximity to the fracture and screw breakage. Proc Inst Mech Eng H 2016;230:599-603.
18. Déjardin LM, Perry KL, von Pfeil DJF, et al. Interlocking Nails and Minimally Invasive Osteosynthesis. Vet Clin North Am Small Anim Pract 2020;50:67-100.
19. Déjardin LM, Lansdowne JL, Sinnott MT, et al. In vitro mechanical evaluation of torsional loading in simulated canine tibiae for a novel hourglass-shaped interlocking nail with a self-tapping tapered locking design. Am J Vet Res 2006;67:678-85.
20. Marturello DM, von Pfeil DJF, Déjardin LM. Evaluation of a Feline Bone Surrogate and In Vitro Mechanical Comparison of Small Interlocking Nail Systems in Mediolateral Bending. Vet Comp Orthop Traumatol 2021;34:223-33.
21. Deprey J, Blondel M, Saban C, et al. Mechanical evaluation of a novel angle-stable interlocking nail in a gap fracture model. Vet Surg 2022;51:1247-56.
22. Guo Z, Sang L, Meng Q, et al. Comparison of surgical efficacy of locking plates and interlocking intramedullary nails in the treatment of proximal humerus fractures. J Orthop Surg Res 2022;17:481.
23. Grzeskowiak RM, Freeman LR, Harper DP, et al. Effect of cyclic loading on the stability of screws placed in the locking plates used to bridge segmental bone defects. J Orthop Res 2021;39:516-24.
24. Hahn JA, Witte TS, Arens D, et al. Double-plating of ovine critical sized defects of the tibia: a low morbidity model enabling continuous in vivo monitoring of bone healing. BMC Musculoskelet Disord 2011;12:214.
25. Mills LA, Simpson AH. In vivo models of bone repair. J Bone Joint Surg Br 2012;94:865-74.

Cite this article as: Koch DW, Johnson JW, Smith QE, Brekhus C, Gadomski BC, Palmer RH, Easley JT, Nelson BB. Biomechanical evaluation of interlocking nail and locking compression plating for stabilization of ovine critical-sized segmental tibia defects. Ann Transl Med 2023;11(6):258. doi: 10.21037/atm-22-4886

